Crystallization of stretched network chains in cross-linked natural rubber

AUTHOR(S):

Tosaka, M; Senoo, K; Kohjiya, S; Ikeda, Y

CITATION:

Tosaka, M ...[et al]. Crystallization of stretched network chains in cross-linked natural rubber. JOURNAL OF APPLIED PHYSICS 2007, 101(8): 084909.

ISSUE DATE:

2007-04-15

URL:

http://hdl.handle.net/2433/50373

JOURNAL OF APPLIED PHYSICS **101**, 084909 (2007)

Crystallization of stretched network chains in cross-linked natural rubber

Masatoshi Tosaka,[a] Kazunobu Senoo, and Shinzo Kohjiya[b]
Institute for Chemical Research, Kyoto University, Gokasyo, Uji, Kyoto-fu 611-0011, Japan

Yuko Ikeda
Kyoto Institute of Technology, Matsugasaki, Kyoto, Kyoto-fu 606-8585, Japan

(Received 2 October 2006; accepted 1 February 2007; published online 23 April 2007)

Relatively fast kinetics of strain-induced crystallization (SIC) of cross-linked samples with various network-chain densities (ν) of natural rubber and its synthetic analog was examined by the fast time-resolved wide angle x-ray diffraction and simultaneous tensile measurements. The lateral crystallite size was almost unchanged with elapsed time, though the crystallization proceeded considerably during the period. The rate of SIC was faster for the samples having the higher ν during the first tens of seconds. While the development of SIC obviously depends on ν, progress of relative stress relaxation with time was almost independent of ν. The different dependence of the experimental results on ν was explained by assuming coexistence of stretched and relaxed network chains. During SIC at a fixed strain ratio, the intensity of crystalline reflections increased without reducing the intensity of anisotropic amorphous halo on the equator. Accordingly, rather relaxed chains that had shown the off-equatorial scattering were thought to be consumed for the crystal growth. © *2007 American Institute of Physics*. [DOI: 10.1063/1.2716382]

I. INTRODUCTION

Strain-induced crystallization (SIC) of natural rubber (NR) has long been the subject of scientific inquiry.[1] The induced crystals are thought to be responsible for the excellent performance of the NR products. Its synthetic analog (*cis*-1,4-polyisoprene rubber: IR) still cannot reproduce the good performance (e.g., crack growth resistance) of the NR products because of slower rate of SIC.[2,3] However, details about the effect of the strain-induced crystals on mechanical properties are still unclear. According to the theory of rubber elasticity, network-chain density (ν) determines the basic mechanical properties such as Young's modulus.[4] The strain-induced crystals would exhibit a secondary effect as filler particles, further increasing the modulus. They could also play the role of additional cross-linking points. (However, the latter effect has not been confirmed experimentally.) At the same time, stress relaxation occurs as a result of SIC,[3,5–11] which apparently reduce the modulus. In order to consider the combination of these effects, a mechanical model representing the rubber network system with strain-induced crystals must be established. Such a mechanical model is essential for the development of advanced rubber materials. For the construction of the mechanical model, morphological features of the strain-induced crystals in relation to the network structure must be specified. At the same time, mutual relationship among deformation, SIC, and mechanical response must be studied.

In this respect, so-called dynamic experiments in which the samples are continuously deformed have been performed.[9,12–23] On the basis of the degree of crystal lattice deformation with nominal stress for samples with various ν, a rough mechanical models has been proposed.[21] However, there still remain matters of opinion for the basic morphological feature of the strain-induced crystals. For example, some researchers assume the strain-induced crystals as aggregates of fully extended network chains, which resemble fringed micell crystals.[24] Other researchers take the shish-kebab structure[24] into consideration. In the latter case, like the crystals of linear-chain polymer, the folded-chain crystals will be included as the constituents of the strain-induced crystals. These two morphologies will lead to different mechanical models, and accordingly, this is an important issue.

For neat NR (before cross-linking), transmission electron microscopy (TEM) revealed that the stretched samples form folded-chain crystals.[25–28] On the other hand, for cross-linked NR, no conclusive evidence of this issue has been presented, although the wide angle x-ray diffraction (WAXD) study[21] and the small angle x-ray scattering study[29] implicitly suggested the formation of folded-chain lamellar crystals. The morphological observations of cross-linked NR by TEM presented the formation of fibrillar structure in the stretched sample, but they also did not afford a conclusive evidence on this issue.[30–32]

Besides the dynamic experiment, studies on kinetics of SIC at a fixed strain ratio are also informative. In this type of study, the sample is expanded to a predetermined strain ratio (α_s), and the development of SIC with time is examined by, e.g., the Avrami analysis. According to the former studies,[6–8] the Avrami exponent changed from ~3 to 1 with the increase in α_s, indicating the change in the growth mode from spherical to aciform crystallization. (In this article, the strain ratio, α, is defined as l/l_0; l and l_0 are the lengths of the deformed and the initial states of the sample, respectively.) When we consider the isothermal experiment at room temperature, the growth mode would be limited to the aciform crystallization,

[a]Author to whom correspondence should be addressed; FAX: +81-774-38-3069; electronic mail: tosaka@scl.kyoto-u.ac.jp
[b]Present address: Faculty of Science, Mahidol University, Salaya Campus, Puthamonthon, Nakorn Pathom 73170, Thailand.

because the strain ratio at the onset of crystallization (α_0) is ~ 3,[20,21,33] at which the growth mode has already changed to the aciform crystallization.[6–8] On the basis of these results, the fringed micell model appears to be more likely for the strain-induced crystals.

A problem on the interpretation of the former kinetic studies[6–8] is the very long time scale of the experiment. In these studies, stress relaxation was evaluated as a measure of crystallization.[6–8] In order to relate the stress relaxation only to SIC, however, one must exclude the effect of plastic deformation. Accordingly, in the former studies,[6–8] the sample was kept at the predetermined strain ratio (α_s) at elevated temperature until the sample was equilibrated, and SIC was initiated by lowering the sample temperature. This procedure restricted the experiments to relatively slow SIC at the small values of α_s; at the large value of α_s, the rate of SIC is too fast to be followed by the measurement of stress relaxation after the equilibration. Thus the length of experimental time ranged from several hours to several months. Such time scales are quite different from the above dynamic studies, and accordingly, different aspects of crystal growth could have been observed. Probably, only the exception has been the thermal study by Mitchell and Meier.[34] After quick expansion of the NR sample, they measured the excess temperature rise, and related it to the degree of SIC. Though this work provided quite significant information for the rapid SIC at high α_s, there was a problem that the data after a few seconds of the deformation could not be used due to dissipation of the heat. Furthermore, only one type of rubber sample has been studied in this work. Accordingly, important issues such as relationship between SIC and stress relaxation or the effects of ν have not been discussed.

In our previous paper,[3] therefore, relatively fast kinetics of SIC for the samples with various ν were examined by the fast time-resolved WAXD and simultaneous tensile measurement. Not only NR but also IR was used as the sample. An interesting outcome was that the stress relaxation behavior with elapsed time after normalization by the maximum stress value (hereafter, we mention this behavior as "the relative stress relaxation") was almost independent of ν. However, reasonable interpretation for the behavior has not been presented.

In this article, for the discussion of the morphological feature of the strain-induced crystals and for the interpretation of the stress relaxation behavior, the experimental data in our previous study[3] were analyzed in more detail.

II. EXPERIMENT

The details of the sample preparation and the experimental procedures have been reported in our previous paper.[3] Ring-shaped samples of sulfur-cross-linked rubber having various ν were used (Table I). The smaller number attached to the sample code corresponds to the larger ν value. The sample was expanded to six times the original length in 12 s and was maintained at the extension during the simultaneous WAXD and tensile measurements. The exposure conditions for the WAXD study are shown in Table II. In order to enable the fast time-resolved WAXD data acquisition (conditions 1 and 2 in Table II), the synchrotron light source at BL-40XU beam line of SPring-8 and a high-speed charge-coupled device (CCD) camera (Hamamatsu C4880-80) were used. For the long exposure experiment (condition 3 in Table II), the CCD camera was replaced with a high-resolution one (Hamamatsu C4880). In the analysis below, the origin of elapsed time (in units of seconds), t, was defined as the moment when the expansion was stopped. That is to say, the expansion started at $t=-12$ s; during $-12<t<0$, the sample has been deformed; the expansion stopped at $t=0$ s. In this article, the SIC behavior after stopping the expansion ($0 \leqslant t$) is mainly discussed.

TABLE I. Cross-linked rubber samples.

Sample code	Network-chain density $\times 10^4$ (mol/cm^3)
NR1	2.12
NR2	1.78
NR3	1.46
NR4	1.31
NR5	1.01
NR9	0.54
NR10	0.37
IR1	1.99
IR2	1.66
IR3	1.36
IR5	1.03

III. DATA ANALYSIS

A. Peak fitting

The quality of the WAXD images was not enough to allow us the discussions on the absolute values of crystallite size, because of the distortion of the WAXD patterns projected on the spherical screen of the CCD camera.[3] Accordingly, we used the width of the diffraction peak as an alternative measure and only the relative changes were considered; the larger value of the width indicates the smaller crystallite size. We selected rectangular regions along the equator of the WAXD pattern, as shown in Fig. 1. Each of the region included 200 or 120 reflection of NR crystals. The intensity values in each region were integrated in the direction parallel to the meridian. Thus we obtained the equatorial diffraction profiles for each of the region including the crystalline reflection. After subtraction of the linear base line, each diffraction profile was fitted by the Gaussian function,

TABLE II. Exposure conditions for the WAXD study.

Condition	Exposure length (s)	Cycle length (s)	Maximum value of t (s)	Applied samples
1	0.036	0.083	8	All
2	0.036	1	30	All except for IR1
3	0.100	30	1800	NR1, NR4, NR5, NR10, IR2, and IR5

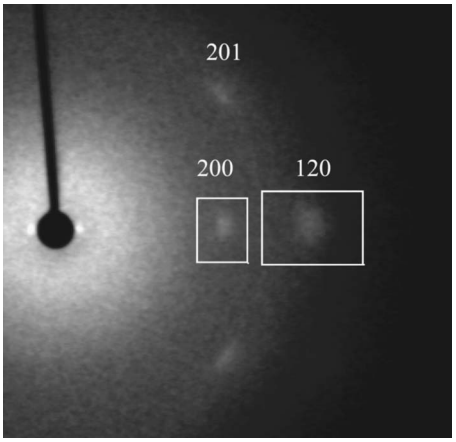

FIG. 1. Major reflections from the oriented crystals in stretched NR4. The rectangular regions indicate the areas selected for the peak fitting of the 200 and 120 reflections.

$$G(x) = h \exp[-(x - x_c)/2w^2], \quad (1)$$

where x is the coordinate in pixel unit, x_c is the position of the peak, and h and w correspond to the height and width of the reflection, respectively. On the basis of the preliminary analysis, x_c was regarded to be constant and only h and w were estimated as fitting parameters. The values of h were normalized by the integrated intensity of the halo on both sides, as in our previous paper.[3] (We have confirmed that the integrated intensity of the halo is almost constant, and accordingly, it can be used as a reference for the normalization.) This procedure was accomplished for hundreds of WAXD data files by using a homemade software. The average values of h and w among a pair of 120 (or 200) reflections were evaluated as measures of crystallinity and lateral crystallite size, respectively. This peak fitting was applied for the data by conditions 1 and 2 in Table II. The samples that presented no or merely weak reflections were excluded from the analysis below because their fitting parameters fluctuated considerably, and furthermore, the discussion on crystal morphology was not applicable for uncrystallized samples.

B. Extraction of anisotropic components

As schematically shown in Fig. 2, the WAXD pattern (Fig. 1) is regarded as the superposition of the isotropic component (isotropic amorphous halo) and the residual anisotropic components (crystalline reflections and oriented amorphous halo). The isotropic component was obtained by connecting the minimum values of the scattered intensity on the azimuthal scans taken at different scattering angles. Then the isotropic component was subtracted from the original WAXD pattern. The residual was regarded as the anisotropic component.[14,16,18,19,21] The WAXD images of the anisotropic component were utilized to investigate the existence of weak scattering from oriented molecular chains.

IV. RESULTS AND DISCUSSION

A. Width of the equatorial reflections

Figure 3 plots the width, w, of the 200 and 120 reflections versus elapsed time, t, for NR samples. (Because of the low intensity of crystalline reflections, the data for IR samples considerably fluctuated. Accordingly, they were excluded from the analysis.) The width values of both reflections fluctuated within ~1 pixel. On the basis of correlation analysis (see Appendix A), we judged that the width of each reflection was almost constant though SIC proceeded considerably for these samples as shown shortly. This result indicates that no significant change in the lateral crystallite size occurs with the progress of SIC.

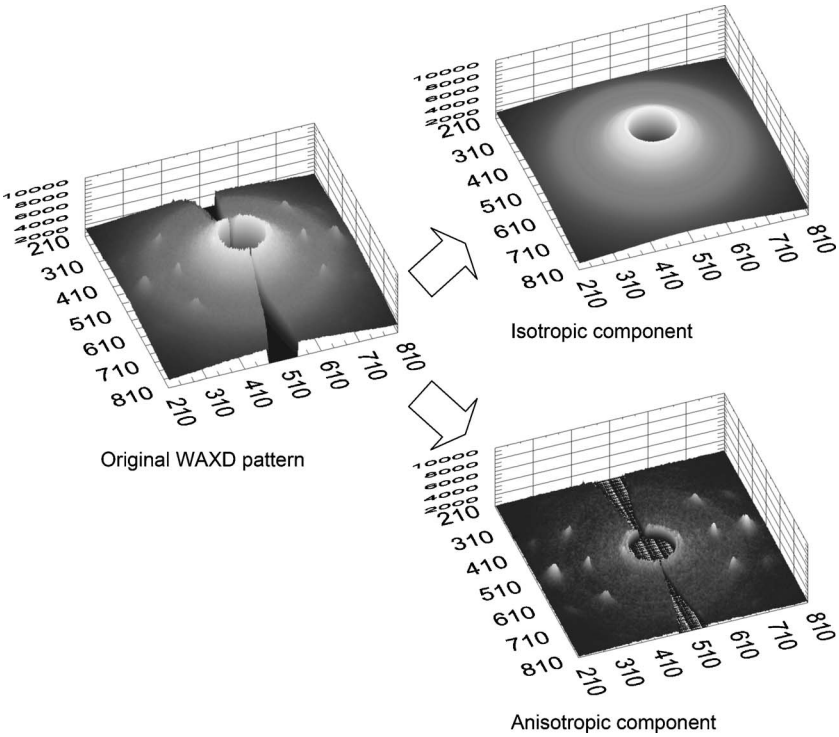

FIG. 2. Schematic representation of the decomposition of the WAXD pattern into isotropic and anisotropic components.

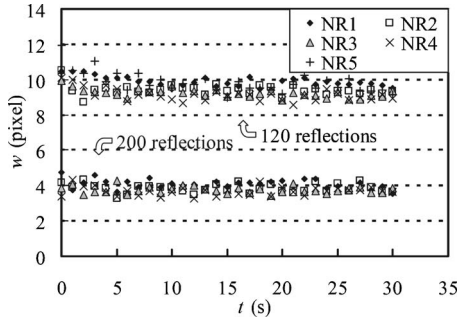

FIG. 3. Variation of peak width, w, with time for NR samples. Only the data for condition 2 are plotted for the better visibility. The data for condition 1 almost overlap the data shown here.

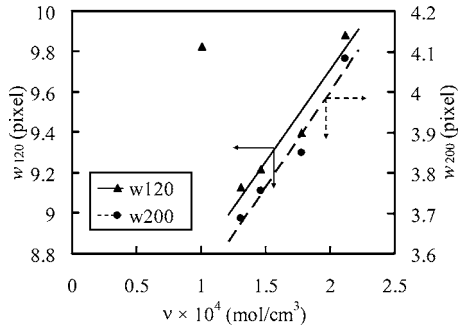

FIG. 4. Time average of peak width, w, as a function of network-chain density, ν. The average values for the 120 and 200 reflections are denoted as w_{120} and w_{200}, respectively.

The w value of the 120 reflection is about twice that of the 200 reflection. This difference of w would be related to the statistical displacement of molecular chains in the crystal structure of NR.[35,36] According to the crystal structure analysis by Nyburg[35] and by Takahashi and Kumano,[36] the molecular chains in the unit cell are statistically replaced with those related by the mirror symmetry at $y=1/8$. By this replacement, projection of the molecular chains on the ac plane, and hence the coherent crystallite size corresponding to the 200 reflection, do not change, while that corresponding to the 120 reflection is reduced. As a result, the breadth of the 200 reflection is smaller than that of the 120 one. The detection of the different w values between the 120 and 200 reflections suggests that our analysis gave, at least qualitatively, correct information concerning the crystallite size, overriding the fluctuation.

In Fig. 3, difference of the w values among the samples with different ν values was not clear due to the fluctuation. Because the w value is regarded to be constant for each sample, its time average was compared to cancel the fluctuation. Figure 4 shows the time averages for the 120 reflections (w_{120}) and for the 200 ones (w_{200}) as a function of ν. There is a clear correlation indicating that the sample with the larger ν has the larger w, and hence smaller crystallite size. This result is consistent with the case of the cyclic deformation experiment,[21] in which the samples with the larger ν showed a smaller crystallite size. Thus we could obtain further information on the morphological features of strain-induced crystals.

B. Progress of strain-induced crystallization

Parts (a) and (b) of Fig. 5 show the peak height of the 120 reflections, $h_{120}(t)$, of NR and IR samples, respectively. Because the scattering mass (thickness × irradiated area) of the sample and width of the reflection, w, are almost constant after stopping the expansion, the intensity value $h_{120}(t)$ can be regarded as a direct measure of crystallinity. In this figure, two sets of data for each sample (conditions 1 and 2 in Table II) are plotted in the range $0<t<8$ s. Because the two sets of data are almost overlapped, the reproducibility of the data is confirmed. On the other hand, there are perceivable fluctuations of the plotted values. Accordingly, we limit the discussion to the overall trends found in this figure.

The rate of SIC (crystallized mass per unit length of time) for NR is obviously faster than IR when we compare the samples of similar ν values, which have the same number in the sample codes. The overall trend for the development of crystalline reflection was consistent with our previous analysis.[3] The peak height for the 200 reflections (not presented in this paper) showed essentially the same trend as in Fig. 5, though the values of h and w were more fluctuated due to the weaker intensity, and hence the smaller signal-to-noise (S/N) ratio, than 120 reflections. As has been discussed in our previous paper,[3] Fig. 5 indicates that the rate of SIC is faster for the samples having the higher ν, which is an opposite trend to the former works under small $\alpha_s(\leqslant 4)$.[6] This fact indicates that we observe different aspects of SIC depending on the time scale of the observation. According to the thermal study by Mitchell and Meier,[34] the time constant of SIC was tens of milliseconds. Their sample (merely one type) was prepared using the same amount of sulfur, and

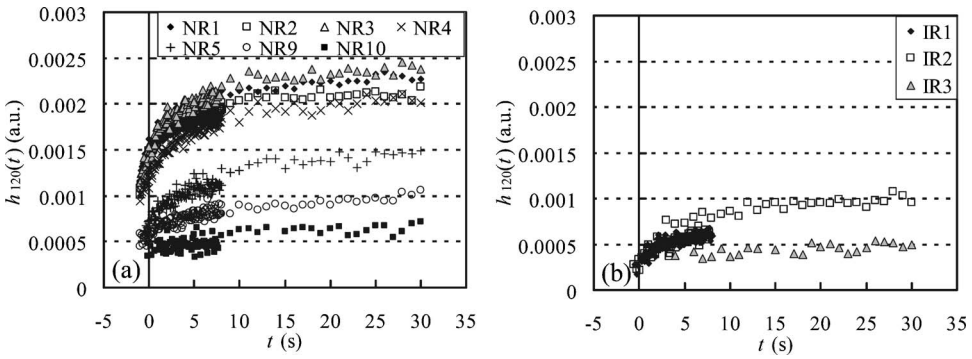

FIG. 5. Variation of peak height with time for 120 reflections of (a) NR and (b) IR samples.

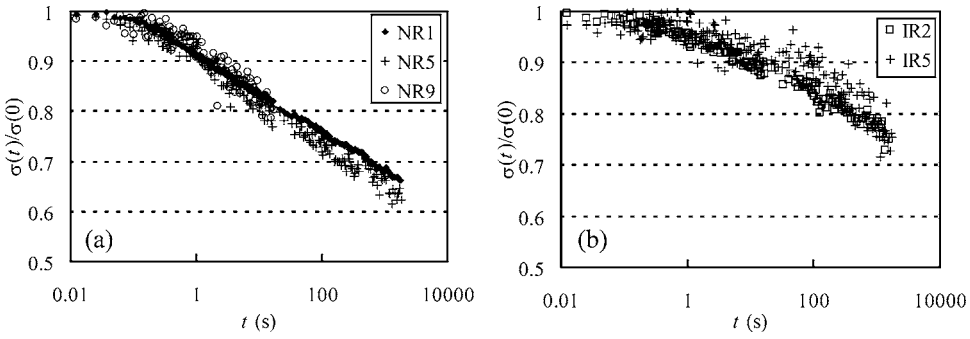

FIG. 6. Normalized tensile stress, $\sigma(t)/\sigma(0)$, for (a) NR and (b) IR. The data from conditions 1–3 in Table II were combined. In order to improve the visibility, some of the data are skipped in the plots.

hence had the similar ν value, with NR3 in our study. In conformity with their work, SIC of NR3 proceeded considerably even during the expansion of the sample [Fig. 5(a)]. Our experiment[3] further clarified that SIC significantly progresses up to 10 s after stopping the expansion. This range of elapsed time has been studied neither by Mitchell and Meier[34] nor by other works concerning the kinetics of SIC.[6–8] Considering the practical usage of rubber products, the data presented in Fig. 5 should be quite significant.

C. Relationship among stress relaxation, strain-induced crystallization, and network-chain density

While the development of SIC obviously depended on ν, the relative stress relaxation with elapsed time was almost independent of ν.[3] Figure 6 shows the stress values after normalization by the maximum stress at $t=0$ s, namely, $\sigma(t)/\sigma(0)$. This type of normalization has been adopted also in the classic studies.[7,8] Only two or three samples are plotted in Fig. 6 for better visibility. The data for other samples are found in our previous paper,[3] in which all the data for each of NR and IR almost overlapped. Because the samples were not equilibrated after the deformation,[6,8] both SIC and plastic deformation must be considered as the origin of the stress relaxation. On this point, we have already shown that the contribution of SIC is dominant.[3] The faster decrease of the relative stress, $\sigma(t)/\sigma(0)$, of NR may be tentatively interpreted as a result of faster crystallization compared to IR.

According to Fig. 5, crystallinity for NR9 and IR2 changed with time in a similar manner,[3] though they have quite different ν values. In this case, the larger ν of IR2 compensated the inherently slower crystallization rate of IR. Now, why are the stress relaxation curves for NR9 and IR2 quite different with each other, though they have almost the same crystallinity? Why is the stress relaxation behavior in Fig. 6 almost independent of ν, though SIC behavior obviously depends on ν (Fig. 5)? If we suppose a uniform network structure, these questions are quite difficult to answer; bulk crystallinity would be directly related to the degree of stress relaxation. On the other hand, if we assume coexistence of stretched and relaxed network chains, we can consistently explain the results in Figs. 5 and 6, as shown below.

At first, the assumption must be justified. There is a characteristic feature in the WAXD pattern of a cross-linked NR sample; even at high expansion, the highly oriented crystalline reflections and strong almost isotropic amorphous halo coexist.[12,14,21,33,37] A quantitative analysis of this feature revealed that the majority of molecular chains are relaxed in almost randomly coiled states, and the residual minor fraction of molecular chains support the applied stress as oriented amorphous and crystal components.[12,14] Formation of fibrillar structures that has been revealed by TEM also supports that only a small fraction of molecular chains are highly stretched.[30–32] Dietrich *et al.*[38] theoretically predicted this situation considering the finite extensibility of the network chains. The differentiation of the network chains into the stretched and relaxed components would result from either the inherently fluctuated network structure[14,33] or the effect of randomly entangled chains.[39] In this way, the assumption, i.e., coexistence of stretched and relaxed network chains, has experimental and theoretical bases.

Figure 7(a) schematically illustrates the molecular trajectories in the stretched rubber sample before the occurrence of SIC. (The inclusion of folded-chain crystals in Fig. 7 will be justified later.) The thick and thin lines indicate the relatively short and long trajectories, respectively. Network chains along the short trajectories are stretched, exhibiting the entropic elasticity, while those along the long trajectories are relaxed. Hereafter, the weak retracting force from the relaxed chains and the minor effect of plastic deformation[3] are ignored for simplicity. The macroscopically measured stress is the sum of the retracting force exhibited by the stretched network chains along the short trajectories. The maximum stress at $t=0$ s, namely, $\sigma(0)$, would be proportional to the number of such short trajectories. Because the samples with the larger ν have the larger number of the short trajectories, they exhibit the larger stress. By noticing that $\sigma(0)$ should be proportional to the number of such short trajectories, the normalized stress value, namely, $\sigma(t)/\sigma(0)$, is interpreted to be a measure of average stress per unit number of the short trajectories. As time passes, the molecular chains along the

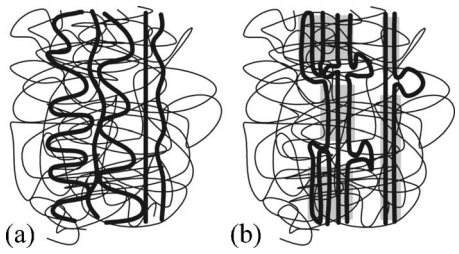

FIG. 7. Molecular trajectories in the stretched rubber sample (a) before and (b) after SIC. The thick and thin lines indicate the relatively short and long trajectories, respectively. The shaded parts designate strain-induced crystals. The cross-linking points are not drawn for simplicity.

short trajectories crystallize [Fig. 7(b)] because of the entropic reason.[21,40] The parts of molecular chains included in the crystals [shaded parts in Fig. 7(b)] should no longer exhibit entropic elasticity and the slack of the chains is excluded from the crystalline part. The amorphous parts of the partly crystallized molecular chains are looser than before. As a result, the stress from each of the stretched trajectory decreases as SIC proceeds.[9,18,21,41,42] Then, the data in Fig. 6 would indicate that the rate of crystallization for the unit number of the short trajectories is almost independent of ν for each of NR and IR. On the other hand, the difference between NR and IR [parts (a) and (b) of Fig. 6, respectively] indicates inherently slower crystallization of the latter molecular chains. Though macroscopic crystallinity is almost the same between NR9 and IR2, if we compare the crystallinity for the unit number of the short trajectories, the former should have the larger value. Accordingly, the stress relaxation curves for these samples in Fig. 6 would be quite different with each other. The idea presented here must be quite important; the crystallinity is not directly related to the relative stress relaxation. The coexistence of stretched and relaxed network chains is regarded as an essential feature for the establishment of the mechanical model of this system. Interpretation of the tensile properties of vulcanized rubber[9] would be affected by considering this feature. If the mechanism of SIC changed with ν, the above interpretation concerning Fig. 6 may be difficult. Accordingly, we assume that the mechanism of SIC is the same regardless of the ν values, at least in the range of this experiment which covers the range of ν for general purpose rubber products.

D. Inclusion of loose network chains into strain-induced crystals

The molecular chains along the short trajectories (indicated by the thick lines in Fig. 7) are, in other words, crystallizable component due to the entropic reason;[21,40] the number of possible conformations for these crystallizable chains must be small enough. However, there may be no requirement for them to be fully stretched chains. What we must consider is the typical degree of slacking of the network chains that can be included into the crystal. Of course, there can be fully stretched chains on which SIC will be initiated. On the other hand, some of the crystallizable chains could be loose enough to form the chain foldings, as shown in Fig. 7(b); the total degree of molecular orientation will increase if they are incorporated into strain-induced crystals. On the contrary, if the highly oriented chains are exclusively included into the crystals, when the sample was macroscopically expanded and held, their amount would be equal before and after crystallization. In this case, the scattering intensity of final crystalline reflections would have been distributed along the equator as streaks before the crystallization. (In other words, the latter situation is the phase transition from the nematic phase to crystal state.) In order to verify the existence of such streaks, the time series of WAXD pattern during SIC was examined. Because the streaks may have relatively weak intensity, isotropic halo was removed from each WAXD pattern and the anisotropic component was examined. Figure 8 shows the anisotropic component from the

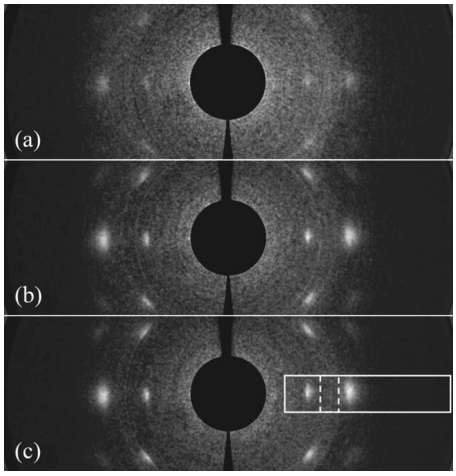

FIG. 8. Anisotropic component of WAXD pattern from NR5 taken at (a) $t=0$ s, (b) $t=60$ s, and (c) $t=150$ s. The rectangular region by solid lines indicate the area used for the estimation of the integrated intensity (halo +reflections) in Fig. 9. The halo intensity in Fig. 7 was estimated for the area between the broken lines.

WAXD patterns of NR5. Because the crystallinity changed from a very small value at $t=0$ s to an easily detectable level, we selected this sample as a representative one. It is noted that this kind of data would not be obtained without the aid of the extremely bright synchrotron x-ray source. We can recognize the increase in the intensity of crystalline reflections, while the streaks from the stretched amorphous chains that would transform into the crystals are not perceptible in the WAXD pattern at $t=0$ s. The integrated intensity on the equator of the WAXD pattern of the anisotropic components (from the area indicated by solid and broken lines in Fig. 8) is plotted in Fig. 9. (These data were taken by condition 3 using the high-resolution CCD camera with the better S/N ratio. The discussion concerning the experimental error in Fig. 9 is presented in Appendix B.) The total intensity on the equator (halo+reflections) is increasing with time, while the intensity of the halo on the equator is almost constant. This figure indicates that increment of the intensity of crystal reflections came from the isotropic and off-equatorial anisotropic scattering. That is to say, rather relaxed chains that had shown the off-equatorial scattering have been consumed for the crystal growth. In other words, Fig. 9 shows that the

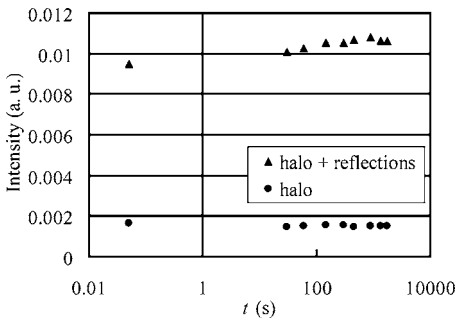

FIG. 9. Variation of integrated intensity on the equator of the anisotropic component of WAXD pattern from NR5. Rectangular areas in Fig. 8 were used for the estimation. Because the data at $t=0$ s cannot be plotted on the logarithmic scale, they are plotted at $t=0.05$ s considering the exposure time of 0.1 s.

overall molecular orientation is enhanced as a result of crystallization. The consensus for the morphology of the strain-induced crystallites in NR is still not achieved. Some researchers illustrate them as fringed-micell crystals. However, we think that the folded-chain crystals should not be ruled out, on the basis of the above results.

V. CONCLUSION

The fast time-resolved WAXD study of the expanded rubber samples showed that the lateral crystallite size was almost unchanged with time, though the crystallization proceeded considerably; the lateral crystallite size was the smaller for the sample with the larger ν. The rate of SIC was faster for the samples having the higher ν, during the first tens of seconds. While the development of SIC obviously depended on ν, relative stress relaxation with time was almost independent of ν. This peculiarly different dependence of the experimental results on ν, both of which are related to the development of SIC, can be reasonably understood if we suppose coexistence of stretched and relaxed network chains. Under this assumption, crystallization rate for unit number of the short trajectories would be related to the normalized stress relaxation, which is almost independent of ν, while the bulk crystallization rate of the whole sample would depend on ν. That is to say, the relative stress relaxation is not directly related to the crystallinity. If this theory holds good, the mechanism of SIC would be the same regardless of the ν values, at least in the range of this experiment.

During SIC at fixed α_s, the intensity of crystalline reflections increased without reducing the intensity of anisotropic amorphous halo on the equator. This result provided the evidence that rather relaxed chains that had shown the isotropic or off-equatorial anisotropic scattering have been consumed for the crystal growth. Accordingly, the folded-chain crystals should not be ruled out for strain-induced crystals.

In this way, we could collect further morphological information for the establishment of the mechanical model representing the rubber network system with strain-induced crystals.

ACKNOWLEDGMENTS

This work was supported partly by a Grant-in-Aid for Scientific Research (B)(2), No. 15404011, from Japan Society for the Promotion of Science, partly by the Research Grants from the President of KIT [to one of the authors (Y.I.)]. The synchrotron WAXD experiments were performed at the SPring-8 with the approval of the Japan Synchrotron Radiation Research Institute (JASRI) (Proposal Nos. 2003B0664-ND1b-np, 2004A0388-ND1b-np, and 2005A0425-ND1b-np).

APPENDIX A

For the data in Fig. 3, we analyzed the correlation between the elapsed time (t) and the width of the reflections (w). As the number of data point is 31, the degree of freedom is 29. In this case, when the absolute value of correlation coefficient (r) exceeds 0.361, the data in question pass the correlation test of 5% of significance level.

Concerning the 120 reflections, the r values ranged between −0.618 and −0.535, indicating the existence of correlation of 5% of significance level, except for NR2 (r= −0.211). The slopes of the regression lines were around −0.02, meaning that w slightly decreases with t when the correlation was confirmed. However, the variation of w with t in our experiment is negligible.

The r values for the 200 reflections ranged between −0.335 and 0.030. As the absolute values of r are smaller than 0.361, correlation between w and t would be negligible. In other words, w would be constant regardless of t.

In this way, whether the correlation between w and t exists or not, we can regard w for each sample to be almost constant.

APPENDIX B

The data in Fig. 9 were derived from the WAXD patterns of anisotropic components in Fig. 2 or Fig. 8. Though the isotropic component (namely, the isotropic halo) has been subtracted, the region near the center appears brighter than the peripheral area. This is due to the relatively large absolute value, and hence fluctuation, of halo intensity near the center compared to the peripheral area (Fig. 2). That is to say, the residual of the halo in Fig. 8 reflects the noise level related to the experimental error. Because the crystalline reflections are clearly recognized in Fig. 8, the reflection intensity is well above the error level. Accordingly, the increase in the intensity (halo+reflections) drawn in Fig. 9 is the phenomenon also above the error level. On the other hand, no streaks are perceptible in Fig. 8. Similarly, the intensity of halo in Fig. 9 is fluctuated around the noise level. That is to say, the halo intensity in Fig. 9 is constant in the range of the experimental error.

[1] J. H. Magill, Rubber Chem. Technol. **68**, 507 (1995).
[2] A. N. Gent, S. Kawahara, and J. Zhao, Rubber Chem. Technol. **71**, 668 (1998).
[3] M. Tosaka, D. Kawakami, K. Senoo, S. Kohjiya, Y. Ikeda, S. Toki, and B. S. Hsiao, Macromolecules **39**, 5100 (2006).
[4] L. R. G. Treloar, *The Physics of Rubber Elasticity*, 3rd ed. (Clarendon, Oxford, 1975).
[5] I. S. Choi and C. M. Roland, Rubber Chem. Technol. **70**, 202 (1997).
[6] A. N. Gent, Trans. Faraday Soc. **50**, 521 (1954).
[7] H.-G. Kim and L. Mandelkern, J. Polym. Sci., Part A-2 **6**, 181 (1968).
[8] D. Luch and G. S. Y. Yeh, J. Polym. Sci., Polym. Phys. Ed. **11**, 467 (1973).
[9] Y. Miyamoto, H. Yamao, and K. Sekimoto, Macromolecules **36**, 6462 (2003).
[10] S. Toki, I. Sics, B. S. Hsiao, M. Tosaka, S. Poompradub, Y. Ikeda, and S. Kohjiya, Macromolecules **38**, 7064 (2005).
[11] S. Trabelsi, P.-A. Albouy, and J. Rault, Rubber Chem. Technol. **77**, 303 (2004).
[12] S. Murakami, K. Senoo, S. Toki, and S. Kohjiya, Polymer **43**, 2117 (2002).
[13] S. Toki, T. Z. Sen, D. Valladares, and M. Cakmak, *Proceedings of the Meeting of the Rubber Division, Providence, RI, 24–27 April 2001* (American Chemical Society, Washington, DC, 2001), Paper No. 12.
[14] S. Toki *et al.*, Macromolecules **35**, 6578 (2002).
[15] S. Toki and B. S. Hsiao, Macromolecules **36**, 5915 (2003).
[16] S. Toki, I. Sics, S. Ran, L. Liu, and B. S. Hsiao, Polymer **44**, 6003 (2003).
[17] S. Trabelsi, P.-A. Albouy, and J. Rault, Macromolecules **36**, 7624 (2003).
[18] S. Toki *et al.*, Rubber Chem. Technol. **77**, 317 (2004).
[19] S. Toki, I. Sics, B. S. Hsiao, S. Murakami, M. Tosaka, S. Poompradub, S. Kohjiya, and Y. Ikeda, J. Polym. Sci., Part B: Polym. Phys. **42**, 956 (2004).
[20] M. Tosaka, S. Kohjiya, S. Murakami, S. Poompradub, Y. Ikeda, S. Toki, I.

Sics, and B. S. Hsiao, Rubber Chem. Technol. **77**, 711 (2004).
[21]M. Tosaka, S. Murakami, S. Poompradub, S. Kohjiya, Y. Ikeda, S. Toki, I. Sics, and B. S. Hsiao, Macromolecules **37**, 3299 (2004).
[22]T. Yoshioka, M. Tsuji, Y. Kawahara, and S. Kohjiya, Polymer **44**, 7997 (2003).
[23]S. Toki, B. S. Hsiao, S. Kohjiya, M. Tosaka, A. H. Tsou, and S. Datta, Rubber Chem. Technol. **79**, 460 (2006).
[24]J. Billmeyer and W. Fred, *Textbook of Polymer Science*, 3rd ed. (Wiley-Interscience, New York, 1984).
[25]E. H. Andrews, Proc. R. Soc. London, Ser. A **277**, 562 (1964).
[26]B. C. Edwards, J. Polym. Sci., Polym. Phys. Ed. **13**, 1387 (1975).
[27]T. Shimizu, M. Tsuji, and S. Kohjiya, Mater. Sci. Res. Int. **4**, 117 (1998).
[28]T. Shimizu, M. Tosaka, M. Tsuji, and S. Kohjiya, Rubber Chem. Technol. **73**, 926 (2000).
[29]D. Luch and G. S. Y. Yeh, J. Macromol. Sci., Phys. **B7**, 121 (1973).
[30]W. F. Reichert, D. Göritz, and E. J. Duschl, Polymer **34**, 1216 (1993).
[31]D. Göritz, Angew. Makromol. Chem. **202/203**, 309 (1992).
[32]D. Göritz, J.-U. Sommer, and E. J. Duschl, Kautsch. Gummi Kunstst. **47**, 170 (1994).
[33]S. Poompradub, M. Tosaka, S. Kohjiya, Y. Ikeda, S. Toki, I. Sics, and B. S. Hsiao, J. Appl. Phys. **97**, 103529 (2005).
[34]J. C. Mitchell and D. J. Meier, J. Polym. Sci., Part A-2 **6**, 1689 (1968).
[35]S. C. Nyburg, Acta Crystallogr. **7**, 385 (1954).
[36]Y. Takahashi and T. Kumano, Macromolecules **37**, 4860 (2004).
[37]J. R. Katz, Naturwiss. **19**, 410 (1925).
[38]J. Dietrich, R. Ortmann, and R. Bonart, Colloid Polym. Sci. **266**, 299 (1988).
[39]R. Everaers and K. Kremer, J. Mol. Model. **2**, 293 (1996).
[40]M. Yamamoto and J. L. White, J. Polym. Sci., Part A-2 **9**, 1399 (1971).
[41]P. J. Flory, J. Chem. Phys. **15**, 397 (1947).
[42]S. Toki, T. Fujimaki, and M. Okuyama, Polymer **41**, 5423 (2000).